5688 *Macromolecules* **2010**, *43*, 5688–5698
DOI: 10.1021/ma100845a

Macromolecules
ARTICLE

Designing Miktoarm Polymers Using a Combination of "Click" Reactions in Sequence with Ring-Opening Polymerization

Kunal Khanna,[†] Sunil Varshney,[‡] and Ashok Kakkar*,[†]

[†]*Department of Chemistry, McGill University, 801 Sherbrooke St. West, Montreal, Quebec H3A 2K6, Canada, and* [‡]*Polymer Source Inc., 124 Avro Street, Dorval (Montreal), Quebec H9P 2X8, Canada*

Received April 20, 2010; Revised Manuscript Received May 27, 2010

ABSTRACT: The design and synthesis of a well-defined molecular building block with three orthogonal functionalities which facilitate the construction of ABC-type miktoarm star polymers via a combination of sequential Cu^{I}-catalyzed cycloaddition of an azide to an alkyne ("click") followed by ring-opening polymerization are reported. Using this simple and highly versatile methodology, a variety of miktoarm star polymers were prepared which consisted of hydrophilic poly(ethylene glycol) and hydrophobic polystyrene and poly(ε-caprolactone) arms. Their self-assembly in an aqueous medium was examined using dynamic light scattering and transmission electron microscopy. These ABC miktoarm polymers were found to self-assemble into spherical micelles whose core size and hydrodynamic diameter were found to be inversely proportional to the size of the PEG arm. The potential of encapsulating small molecules into these micelles was explored using Disperse Red 1 dye. An enhancement in the loading capacity of the micelles was observed with an increase in the length of the hydrophobic arm.

Introduction

Miktoarm polymers[1] constitute an intriguing class of star-shaped polymers whose arms can be varied in terms of their chemical identity and/or molecular weight.[2] The inherent architecture of these polymers that can be finely tuned based on the desired features and their unique self-assembly[3] has made this relatively novel class of macromolecules very attractive for applications in a large variety of areas, the most widely explored of which are micellization and drug delivery.[4] The challenges that were faced in the preparation of these star polymers using earlier techniques such as living anionic polymerization and chlorosilane chemistry have led to the development of some elegant synthetic methodologies,[5] including "arm-first",[5k] "core-first",[5l] "in−out",[5m] and coupling,[5n] each with its own merits. Despite requiring the synthesis of a unique small molecule designated as the core of the star structure, coupling methods have recently garnered much momentum in the field of miktoarm star polymer synthesis because of two important factors: the opportunity to ensure the integrity of each polymer arm before attachment to the growing miktoarm star, and the well-defined control that is achieved over the final structure's number of arms and their chemical identity. Recent addition of "click" chemistry[6] to macromolecule synthesis has provided a highly useful tool to the polymer chemist in diversifying the synthetic strategy of these star polymers. A "click" reaction such as the Cu^{I}-catalyzed cycloaddition of an azide to an alkyne[6a] can be carried out with great ease in a variety of experimental conditions without interfering with a large variety of functionalities that may be present in the overall structure. This reaction has been widely employed in the synthesis of branched macromolecular structures including dendrimers[6b−d] and star polymers.[7]

As it is well documented now, the controlled introduction of different types of polymeric arms onto a single scaffold necessitates a combination of synthetic methodologies in order to ensure the integrity of the final structure. Thus, it is essential to design a core structure with orthogonal functional groups that will allow stitching of polymers at different junctures throughout the synthesis. We report here the construction of a versatile core structure with three orthogonal functionalities that facilitates performing two "click" reactions in sequence, followed by ring-opening polymerization. We used this methodology to construct a library of ABC-type miktoarm star polymers containing a combination of poly(ethylene glycol) (PEG), polystyrene (PS), and poly(ε-caprolactone) (PCL). These linear polymeric arms[8] offer tunability in terms of the properties of the corresponding miktoarm polymers.

The synthetic elaboration of these multicomponent macromolecules has also intrigued scientists to evaluate their self-assembly in solution. Hadjichristidis et al. have carried out numerous studies in which they have shown that the morphologies of the self-assembled structures from miktoarm polymers can range from lamellar to cylindrical structures.[9] In addition, the formation of spherical micelles that were pH-responsive was reported by Babin et al. using A_2B-type miktoarm polymers.[10] Lodge's group has demonstrated that ABC-type miktoarm polymers containing poly(ethylethylene) (PEE), poly(ethylene oxide (PEO), and poly(perfluoropropylene oxide) (PFPO) form multicompartment micelles in aqueous solutions.[11] The aqueous self-assembly of these ABC star polymers was found to be dependent on the individual lengths of the chains and was reported to be dictated by the inherent incompatibility of the polymeric arms. The miktoarm polymers that do not contain such distinct partitions in interactions of their polymeric arms offer another platform to finely tune their self-assembly behavior.[12] We have studied the aqueous self-assembly of ABC μ-miktoarm polymers reported here that contain PEG, PS, and PCL arms, using dynamic light scattering (DLS) and transmission electron microscopy (TEM). These star polymers assemble into spherical micelles, and our results suggest that the size of the hydrophilic corona arm influences the hydrodynamic diameter of the micellar assemblies. We have also evaluated loading of Disperse Red 1 dye molecules into the self-assembled structures of these miktoarm polymers in solution, whose loading efficiency was found to be dependent on the length of the hydrophobic polymeric arms.

Results and Discussion

We first envisioned the construction of a versatile multifunctional core structure on which a variety of miktoarm star polymers (μ-stars) could be easily constructed using a desired

*Corresponding author. E-mail: ashok.kakkar@mcgill.ca.

 Published on Web 06/09/2010

Scheme 1. Synthesis of the Core Compound 4 with Three Orthogonal Functionalities

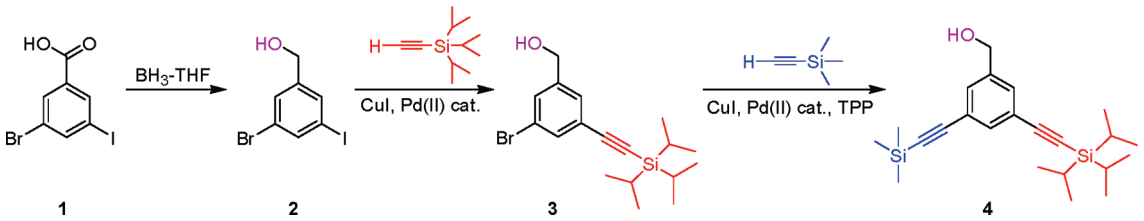

variation of synthetic strategies. One of the key features required in the design of the core structure was the introduction of orthogonality because it ensures a controlled introduction of polymeric arms. By allowing each of its specific functional groups to be activated for the attachment or growth of an individual polymeric arm, the final μ-star can be synthesized with relative ease and minimal purification strategies. While many different "click" reactions have now been identified,[6] the most widely used to date has been the Cu^{I}-catalyzed Huisgen [3 + 2] cycloaddition between an azide and an alkyne (CuAAC).[6a] Some of the key features of this methodology include benign reaction conditions, high yield, relatively simple purification methods, and modular applicability. Many examples have recently surfaced throughout macromolecular chemistry where "click" chemistry has been employed as a synthetic route[6,7] and has been utilized to adjoin building blocks together in a predictable and efficient fashion. To implement the synthesis of ABC-type miktoarm star polymers reported here, compound **4** (Scheme 1) was designed as a core which features (i) a benzylic alcohol that can be used for the ring-opening polymerization of ε-caprolactone and (ii) two protected alkyne groups for "click" chemistry using CuAAC. It is well-known that the trimethylsilyl (TMS) moiety can be selectively cleaved from the protected acetylene under mildly basic conditions, while the remaining triisopropylsilyl (TIPS) moiety is left intact. The latter requires stronger basic conditions for deprotection of its acetylene, thereby ensuring that these two protected acetylenes are orthogonal to one another.[13] Thus, the core structure **4** is a trifunctional compound that can be utilized for two "click" reactions sequentially, followed by ROP to construct a μ-star.

The synthesis of the core started with the reduction of commercially available 3-bromo-5-iodobenzoic acid (**1**) to its corresponding alcohol[14] **2** in high yield (Scheme 1) and was easily monitored via ^{1}H NMR by the appearance of the CH_2−OH group at 4.63 ppm. The Sonogashira coupling reaction was subsequently utilized to covalently link triisopropylsilylacetylene with the aryl iodide group, leading to the synthesis of **3**. It was followed by the appearance of the triisopropylsilyl (TIPS) group in the ^{1}H NMR at 1.12 ppm. In this step, column chromatography was found to be essential for isolation of the monosubstituted compound from the impurities, including the disubstituted side product. The final step in the synthesis involved another Sonogashira coupling reaction between trimethylsilylacetylene and the aryl bromide to yield **4**. Once again, ^{1}H NMR made it easy to confirm this coupling in which the desired TMS group appeared at 0.23 ppm. It should be noted that throughout each of these transformations the changes in the position of the aryl protons in the ^{1}H and ^{13}C{^{1}H} NMR spectra are highly diagnostic for determining the purity of the final compound, as the impurities such as leftover reactants that did not undergo coupling can be easily observed, particularly in the aryl region of the spectra.

The azide-terminated polymers used for "click" reactions with the core were subsequently synthesized (Scheme 2). Poly(ethylene glycol) monomethyl azide (PEG-N_3) **5a** or **5b** was prepared starting from commercially available poly(ethylene glycol) monomethyl ether with $M_n \sim 775$ or 2000 g/mol by adaptation of a literature method.[15] In a general procedure for the synthesis of the azide-terminated polymers, the terminal alcohol in poly(ethylene glycol)

Scheme 2. Synthesis of Monofunctional Azide- and Alkyne-Terminated Polymers 5 and 6

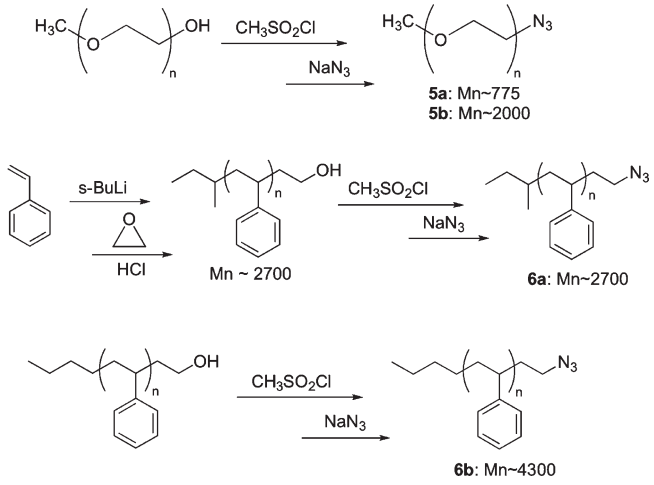

monomethyl ether was quantitatively converted to a mesyl group. The latter is an excellent leaving group for its subsequent nucleophilic substitution with an azide. Polystyrene azide (PS-N_3) of $M_n \sim 4300$ (**6b**) was synthesized in a similar manner from its commercially available monohydroxy form. PS with $M_n \sim 2700$ (**6a**) was synthesized by living anionic polymerization with *sec*-butyllithium as the initiator, end-capped with ethylene oxide. Conversion to its azide form was achieved in a similar fashion as described for **5** and **6a**.[16] It should be noted that ^{1}H and ^{13}C{^{1}H} NMR spectra were found to be highly useful in monitoring the conversions in these reactions.

A general procedure for the synthesis of μ-star polymers using a combination of "click" reactions in sequence followed by ROP is described in Scheme 3 for μ(PEG_{2000}-PS_{4300}-PCL_{4000}: the subscript corresponds to M_n). The details of this methodology apply to the rest of μ-stars synthesized using this route. The synthesis was begun by carrying out "click" reactions, and the conversion of **4** to **7** was the first step for the buildup of miktoarm polymer. Because the integration and peak position of the aryl protons, triazole ring protons, and the acetylene proton become diagnostic in monitoring the reaction, we decided to delay the ROP to the final step in order to facilitate this analysis via ^{1}H NMR. Aqueous potassium carbonate was used to deprotect the TMS group while leaving the TIPS group completely intact, as confirmed by ^{1}H and ^{13}C{^{1}H} NMR. In the ^{1}H NMR spectrum, both the shift in the peak positions of the aryl protons and their relative integration with the new acetylene peak were used to confirm the identity of **7**. The subsequent CuAAC "click" reaction between **5b** and **7** using CuBr/PMDETA as a catalyst yielded compound **8**. The latter reaction was monitored by ^{1}H NMR in which shifts of the core's aryl protons, disappearance of the alkyne proton, and appearance of the PEG chain protons and triazole ring proton were observed. Furthermore, GPC analysis showed a polydispersity (PDI) which was in agreement with the precursor PEG-N_3. Tetrabutylammonium fluoride (TBAF) was subsequently used to deprotect the second acetylene to give

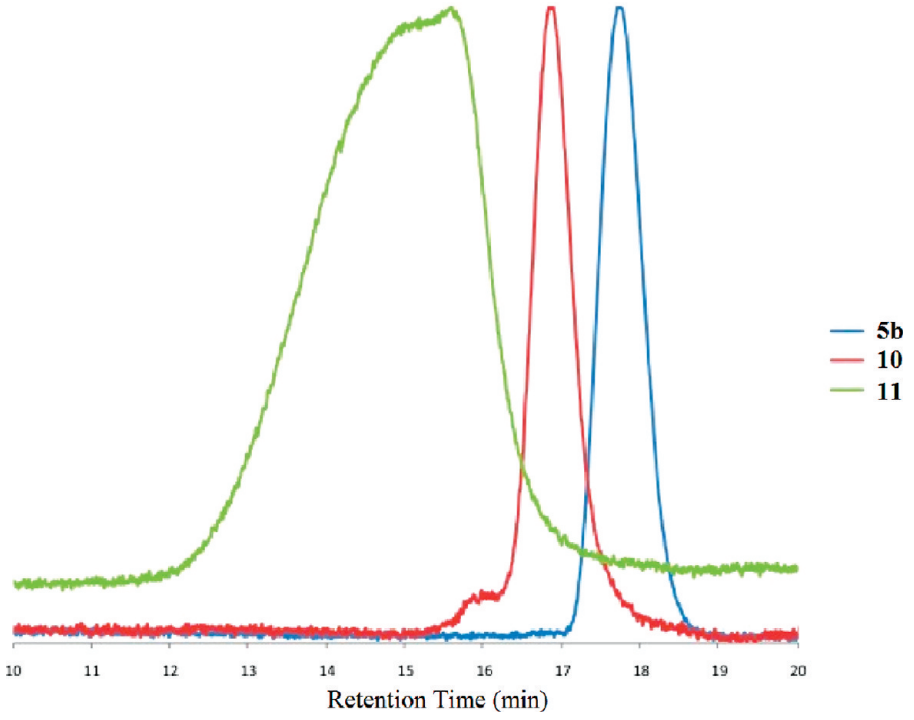

Figure 1. GPC analyses of (a) azide-terminated PEG_{2000}, (b) PEG_{2000}-*b*-PS_{4300} copolymer, and (c) μ(PEG_{2000}-PS_{4300}-PCL_{4000}) ABC miktoarm star terpolymer.

Scheme 3. Synthesis of ABC Miktoarm Star Polymers μ(PEG-PS-PCL) Using CuAAC "Click" Reactions in Sequence, Followed by Ring-Opening Polymerization (ROP)

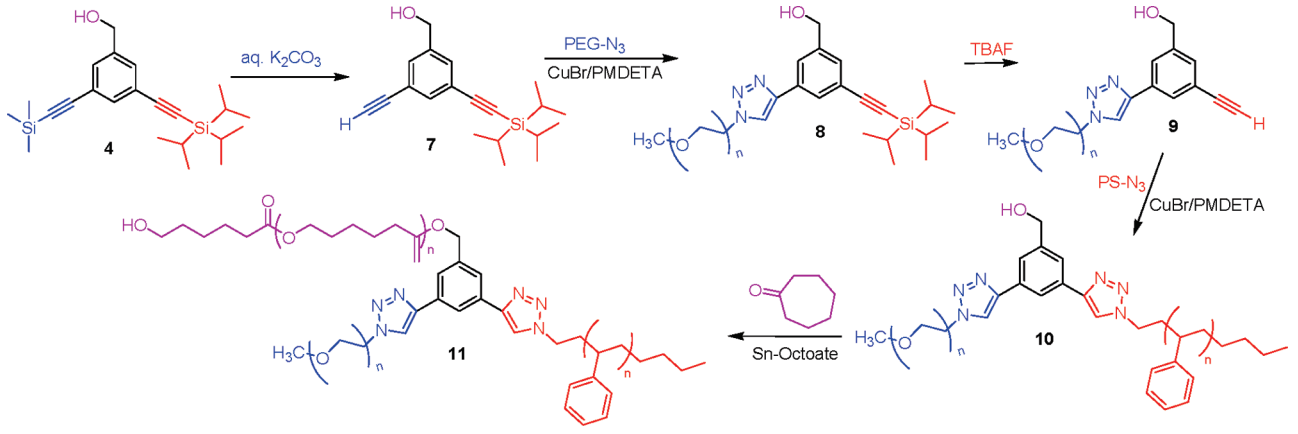

compound **9**. The evidence for this conversion was obtained from peak integration of the new acetylene peak to the aryl protons in ^{1}H NMR, loss of the TIPS group, and the corresponding shifts in the acetylene carbons in $^{13}C\{^1H\}$ NMR.

PEG−PS precursor **10** was synthesized by CuAAC reaction of **6b** with **9**. GPC analysis of the latter showed a complete shift in the chromatogram of the growing μ-star as well as a PDI and molecular weight consistent with both polymeric precursors **6b** and **9**. The macroinitiator **10** was then employed for ROP with ε-caprolactone monomer catalyzed by stannous octoate. The product was precipitated into cold methanol to yield the final μ-star **11** as a white solid. GPC analysis (Figure 1) showed a clear shift in the chromatogram with an increase in molecular weight that corresponded with the theoretical molecular weight based on the monomer/initiator ratio, indicating that an ABC miktoarm star polymer was formed (as opposed to a mixture of macroinitiator **10** and poly(ε-caprolactone) homopolymer). The ^{1}H NMR depicted a new set of peaks that corresponded to poly(ε-caprolactone) (PCL), and the final ^{1}H NMR spectrum of the miktoarm polymer displayed characteristic resonances for each of the three polymeric arms (Figure 2). The μ-star polymers synthesized using this procedure are summarized in Table 1. The PDI of these polymers increased in direct proportion to the desired molecular weight of the PCL arm and is related to the ROP method employed for the synthesis. Such an increase in PDI from the ROP of ε-caprolactone has been reported in the literature. For example, the growth of ε-caprolactone using the same catalyst on a diblock copolymer precursor led to an ABC miktoarm polymer with a broad molecular weight distribution (PDI 1.50).[17] It should be noted that the ROP of ε-caprolactone was conducted at 130 °C except for **14**, where it was first attempted at a more modest temperature of 100 °C. In the latter case, no change in molecular weight was observed when polymerization reaction was performed overnight. After subsequently increasing the reaction temperature to 130 °C, an increase in molecular weight was observed, corresponding to the growth of PCL. This result strongly suggests a slow ROP initiation due to steric hindrance in the diblock miktoarm polymer, which can simply be overcome by performing the

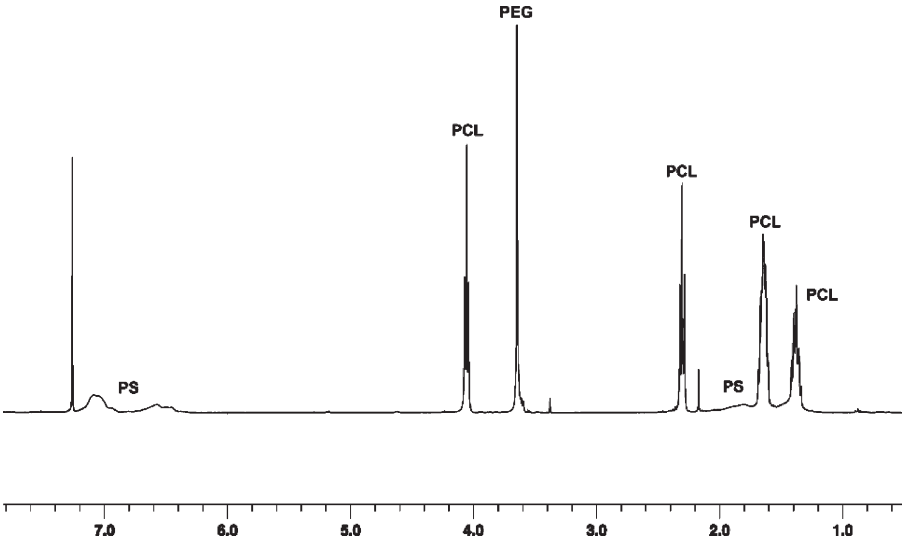

Figure 2. ^{1}H NMR spectrum (400 MHz) of the miktoarm polymer **11** in $CDCl_3$.

Table 1. μ-Star Polymers Synthesized Using Two Sequential "Click" Reactions Followed by ROP

μ-star polymer[a]	compound	PDI[b]	mean D_H of aqueous micelles	mean D_H of DR1 loaded micelles	DR1 loading (wt %)
μ(PEG_{2000}-PS_{4300}-PCL_{4000})	**11**	1.26	185	217	1.3
μ(PEG_{2000}-PS_{4300}-PCL_{10000})	**12**	1.43	118	157	N/A
μ(PEG_{775}-PS_{4300}-PCL_{4500})	**13**	1.40	224	198	1.8
μ(PEG_{775}-PS_{4300}-PCL_{10000})	**14**	1.59	250	222	2.1
μ(PEG_{775}-PS_{2700}-PCL_{3000})	**15**	1.28	212	164	0.4
μ(PEG_{775}-PS_{2700}-PCL_{6900})	**16**	1.55	251	262	1.0

[a] Numbers in subscript indicate M_n of the polymeric arm. [b] From GPC measurements (THF) calibrated with polystyrene standards and refractive index detector.

polymerization reaction at higher temperature. This might explain the increase in polydispersity upon growth of PCL, as it well-known that higher reaction temperatures in ROP generally lead to higher polydispersities.

Self-Assembly of Miktoarm Polymers. We subsequently examined aqueous self-assembly behavior of the library of ABC miktoarm polymers. Aqueous micelle preparation for miktoarm polymers **11** and **12** was carried out by either (i) direct dispersion, i.e., by dissolving a known amount of the polymer in water, or (ii) a dialysis method in which the polymer is dissolved in a solvent compatible with all polymeric arms, followed by addition of water, and finally removal of the solvent by dialysis. Direct dispersion of the polymer into water allowed **11** to self-assemble into micelles, while **12** precipitated out of solution and showed no micellar behavior. On the other hand, both polymers formed micelles in the dialysis technique and even demonstrated reproducibility in the micellar sizes. Therefore, all aqueous micelles were subsequently prepared by the dialysis method, where the polymer was dissolved in 10 mL of a 1:9 ratio of DMF and Milli-Q water (0.1 wt % in solution), and then dialyzed against DMF to yield aqueous micelles. The miktoarm polymers reported here are expected to assemble in aqueous solution so that PEG (a hydrophilic polymeric arm) forms a corona, as it interacts with the surrounding solvent. This protects the hydrophobic interior that is composed of PS and PCL arms which do not interact favorably with water. We examined this behavior using ^{1}H NMR of **11** in D_2O, which confirmed this hypothesis,[18,19] and the ^{1}H NMR showed the peaks for PEG, while the PS and PCL signals were found to be absent due to restricted movement of these polymer arms within the micelle core.

The sizes of aqueous μ-star were examined by dynamic light scattering (DLS), and in general, the polydispersities of the micelles were relatively narrow ($\leq$0.1). It suggested that these star polymers form well-defined assemblies with a fairly narrow size distributions. A comparison of the DLS data for the miktoarm polymers (Table 1) indicated that there may be an inverse relationship between the length of the PEG arm and the mean hydrodynamic diameter (D_H), a trend similar to one observed by other groups.[11a] For example, as the PEG length decreased in going from **12** (PEG_{2000}-PS_{4300}-PCL_{10000}) to **14** (PEG_{775}-PS_{4300}-PCL_{10000}), the mean D_H increased from 118 to 250 nm (Figure 3). Similarly in the case of **11** (PEG_{2000}-PS_{4300}-PCL_{4000}) and **13** (PEG_{775}-PS_{4300}-PCL_{4500}), D_H increased from 185 to 224 nm (Figure 4). We exercise caution in the interpretation of the above results because the miktoarm polymers reported here span a narrow spectrum of PEG volume fractions (f_{PEG}), and therefore any inverse relationship does not take into account different packing motifs that can be observed across a wider spectrum of f_{PEG}.[11a,d] Our correlation between PEG arm size and D_H will need to be further elaborated with polymers that are more hydrophilic than those used in this study. A variety of polymeric systems are currently being explored in numerous laboratories for chemotherapeutic drug delivery with the eventual goal of improving passive targeting of macromolecules toward tumors. It has been suggested[20] that not only can the branched architecture of miktoarm polymers inhibit renal filtration and promote prolonged blood circulation, but higher molecular weight (and, more importantly, the consequent increase in D_H) can also contribute to these beneficial effects. For the miktoarm polymers reported here, shorter PEG arms lead to higher D_H while the overall discrete micellar structure in solution is maintained (see Figures 5−8), suggesting that tuning the size of the overall self-assembled miktoarm polymers may be possible in a way that can help optimize the passive targeting of these macromolecules into tumor tissues.

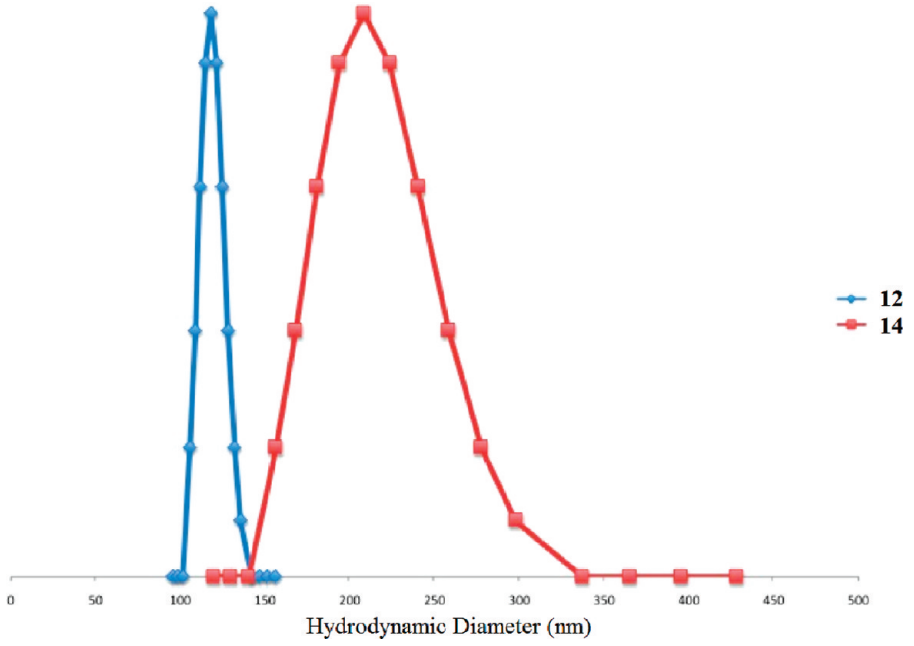

Figure 3. Comparison of hydrodynamic diameter D_H of **12** with **14** in aqueous solution.

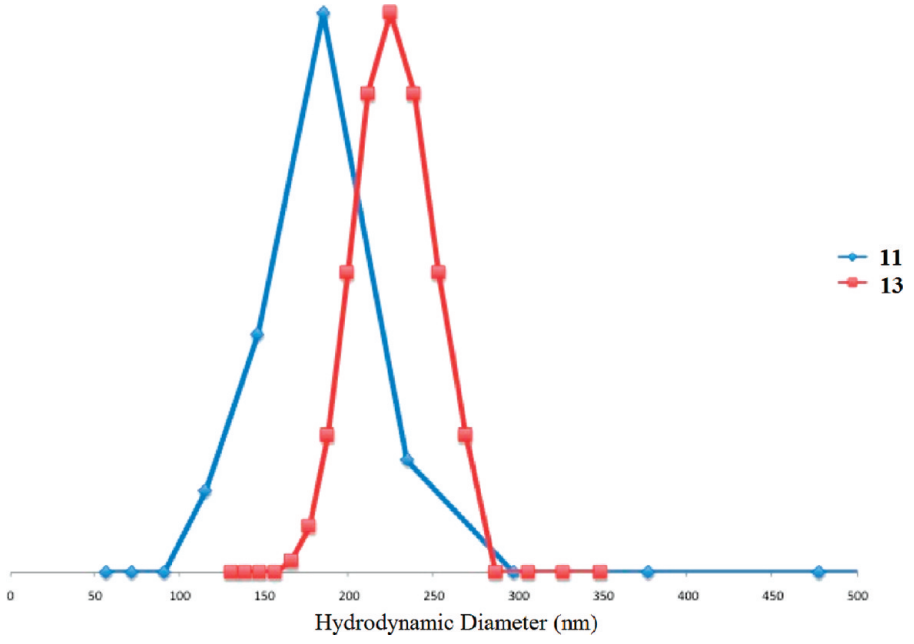

Figure 4. Comparison of hydrodynamic diameter D_H of **11** with **13** in aqueous solution.

Transmission electron microscopy (TEM) was subsequently employed to further elucidate the self-assembly of these miktoarm polymers. In the case of star polymer **11** small, spherical micelles of 10−20 nm in size were observed (Figure 5). One possible explanation here for the disparity between TEM and DLS data, which had given a mean size distribution of 185 nm, lies in the fact that DLS creates a size distribution curve from solvated micelles where the PEG chains, which form the corona, are spread out. On the other hand, TEM images are acquired from dried solutions where the PEG chains are coiled and bent. Additionally, PEG chains will not be visible through TEM, so the sizes obtained from TEM are more representative of the core of the micelles, which is composed of PS and PCL and shows up clearly in TEM.

Self-assembly of **12** in TEM yielded individual micelles with a predominant size distribution between 50 and 100 nm (Figure 6), while DLS had suggested a size distribution of 100−135 nm. Once again, the difference in DLS and TEM data can be attributed to both the lack of solvation of the hydrophilic PEG corona as well as the lack of visibility of these chains. An interesting trend was noted while comparing DLS and TEM data for **11** and **12**. Polymers **11** and **12** differ in the length of the hydrophobic PCL arm which comprises the core. It is 2.5 times larger for **12** compared to **11**, and we observed a corresponding increase in the size of micelles from **12** when examined using TEM. We expect that a similarly proportional increase in size would be measured by DLS, as the only difference between **11** and **12** would be the increase in the size of the core. However, according to

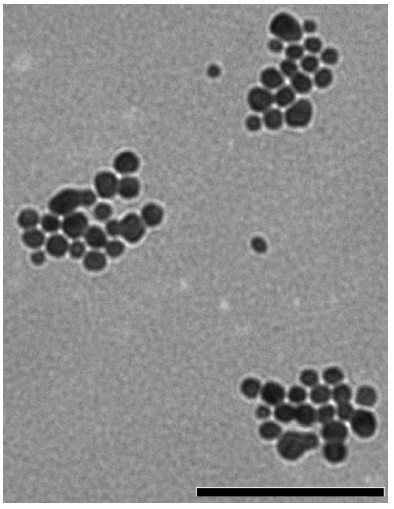

Figure 5. TEM image for micelles of **11**. Scale bar is 100 nm.

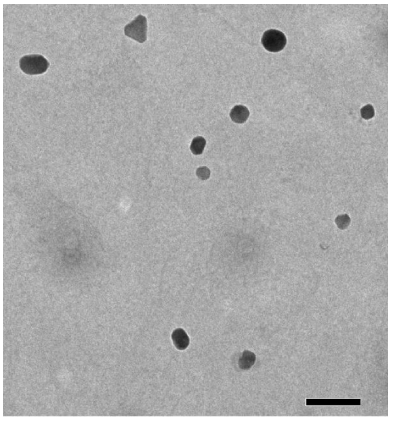

Figure 6. TEM image for micelles of **12**. Scale bar is 500 nm.

DLS results, the micellar size of **12** is significantly smaller than **11**. This suggests that an increased micellar core size which results from longer hydrophobic PCL arms accompanies a change in the structure of the corona where the hydrophilic PEG chains are of the same size. This could be a result of a change in the interfacial curvature of the micelle. In addition, an increase in polydispersity could also contribute to the decrease in D_H observed by DLS. An altogether different chain packing motif could also explain this phenomenon, especially when one considers the limitations that accompany viewing aqueous micelles by TEM.

Miktoarm polymer **13** depicted spherical micelles in TEM (Figure 7), ranging in size from roughly 160 to 250 nm. The size distribution curve from DLS studies of this polymer was found to be between 190 and 270 nm. We attribute the observed TEM sizes to the formation of individual micelles rather than any micellar clusters, based on the excellent baseline fitting from DLS and reproducibility of this data. It is expected that the difference in the size distribution between DLS and TEM should not be as dramatic for polymers **13**−**16** since the PEG chain is almost 3 times shorter, in comparison to **11** and **12**. Thus, a small increase in the micelle size for polymers **13**−**16** is expected when comparing results from TEM to those from DLS. This is confirmed above by a modest increase in size distribution of **13** from TEM (160−250 nm) to DLS (190−270 nm).

It was interesting to compare the micellar core size distribution obtained from TEM studies of star polymers **11** (10−20 nm) and **13** (160−250 nm). It suggested that a dramatic increase in the size of the core can be obtained from a simple decrease in the length of the hydrophilic PEG chain which forms the corona. Similarly, a comparison of the sizes of **12** and **14** (Figure 8) also suggested an inverse relationship between PEG arm length and the size of the core. This trend corresponds with that which was observed from DLS: that controlling the size of the hydrophilic PEG arm allows one to control the size of the micelle. While one may expect a similarity in the core sizes between the micelles of these miktoarm polymers on account of their similarities in sizes of the hydrophobic blocks, it has also been documented that morphological changes within the micellar core can occur as the hydrophilic polymer length is varied.[11a]

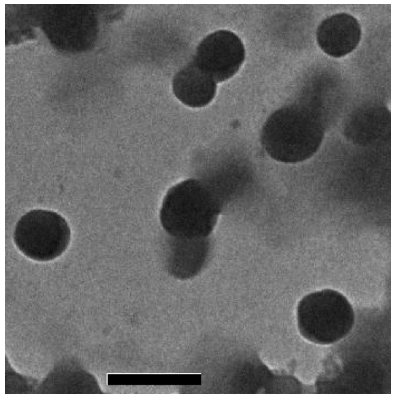

Figure 7. TEM image for micelles of **13**. Scale bar is 500 nm.

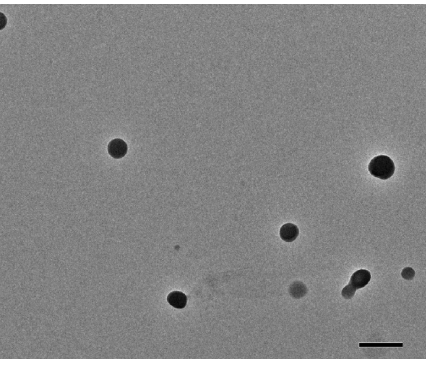

Figure 8. TEM image for micelles of **14**. Scale bar is 500 nm.

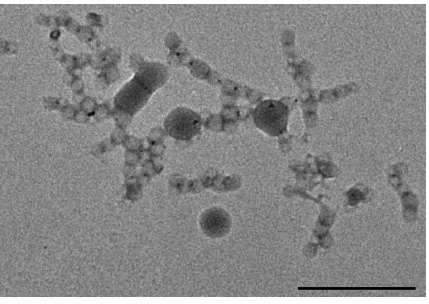

Figure 9. TEM image for micelles of **16**. Scale bar is 500 nm.

Polymer **16** showed a rather unique assembly of micelles that had conjoined from end to end to form an aggregate which resembled a pearl necklace (Figure 9), composed mostly of small micelles (~60 nm). These individual micelles assembled to form aggregates with sizes well over 200 nm. The appearance of large aggregates composed of small

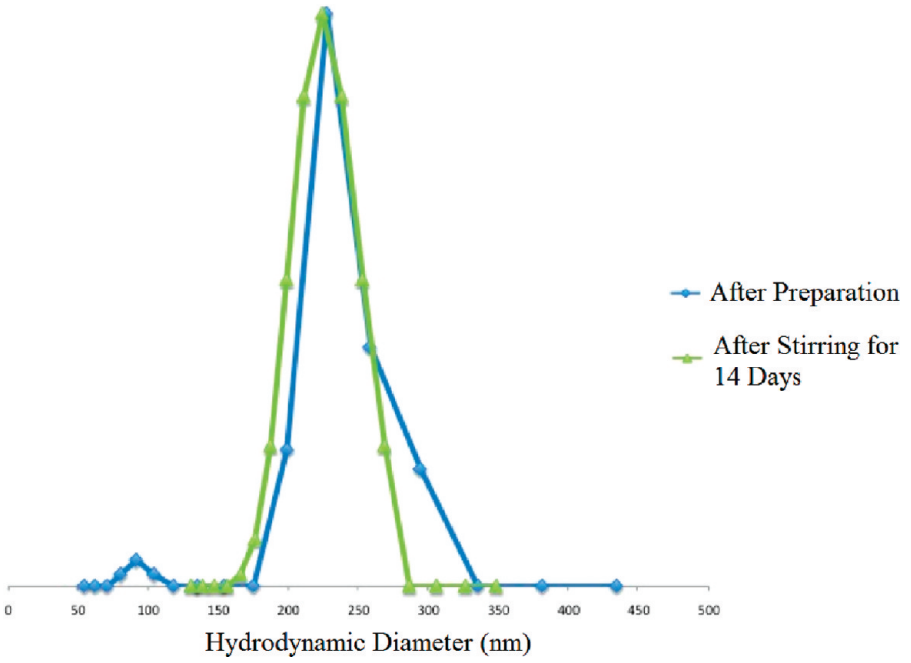

Figure 10. Evolution of size-distribution curve for aqueous micelles of **13**, from micelle preparation through 2 weeks.

micelles helps to explain the predominant population observed in DLS of structures above 200 nm.

Stability of the micelles is highly essential for applications including drug delivery, catalysis, etc. To examine the stability of the micelles formed by miktoarm polymers reported here, DLS data were obtained over a period of 2 weeks. During this period, aqueous micelles were stirred at room temperature. Figure 10 shows data for a representative miktoarm polymer **13**. It showed no significant change in the size of the micelles, suggesting that the micelles were stable once formed in water. Any variations in sizes (within 10 nm) can be attributed to slight changes in temperature or even statistical variations in the data. Nonetheless, the curve for the size distributions retained the same overall shape.

Disperse Red Encapsulation. The encapsulation of small molecules into the assemblies of the miktoarm polymers reported here was evaluated using Disperse Red 1 (DR1). It was considered to be a suitable candidate for this study due to its hydrophobic nature which should facilitate its encapsulation within the hydrophobic core of aqueous micelles. In addition, DR1 does not dissolve in water but has excellent solubility in organic solvents. Thus, upon interaction with aqueous micelles, DR1 would prefer to move into the protected hydrophobic interior of the polymeric micelles, where it will be shielded from unfavorable interactions with the surrounding solvent. Encapsulation was achieved by the extraction technique, where an aqueous polymer solution was stirred with a concentrated solution of Disperse Red 1 in *tert*-butyl methyl ether overnight at room temperature. After allowing the solution to settle for an hour, the aqueous fraction was withdrawn and analyzed by DLS and UV−vis spectroscopy, and the results are presented in Table 1. *tert*-Butyl methyl ether was chosen for the organic phase due to the insolubility of the μ-stars in this solvent.

In general, the DR1-loaded micelles were found to be stable based on the DLS results. The initial size distribution of DR1-loaded micelles was found to be well-maintained upon prolonged exposure to the organic dye solution (for 1 week, Figure 11). Furthermore, this size distribution was maintained through equilibration of the aqueous solution and even upon vigorous stirring of the aqueous solution at room temperature for 2 weeks.

Since we had carried out DR1 loading using the extraction method, a change in hydrodynamic diameter observed upon small molecule encapsulation could be misleading. For example, in a control experiment, we evaluated the changes in micellar size upon exposure to *tert*-butyl methyl ether without the addition of DR1. The aqueous micelles from miktoarm polymers were extracted with *tert*-butyl methyl ether and studied using DLS. The hydrodynamic diameter was found to increase by about 70 nm upon exposure to *tert*-butyl methyl ether. The change in hydrodynamic diameter upon loading the micelle with the dye is of less importance than the stability of the dye-encapsulated micelle itself, as this stability is a more salient feature in the design of a drug delivery nanoparticle.

UV−vis spectroscopy was subsequently employed to quantify the loading capacity of dye molecules within the hydrophobic interior of these aqueous micelles. DR1 solutions in dichloromethane were used to create a calibration curve in order to determine the amount of DR1 that was encapsulated within each micellar system. The calibration curve had a correlation of 99.6%. The dye-encapsulated micelles were lyophilized and harvested into DCM and analyzed by UV−vis spectroscopy. Encapsulation results obtained from this calibration curve are summarized in Table 1, and in general a modest loading between ~1 and 2 wt % was observed. In miktoarm polymer **12**, DR1 loading could not be determined with certainty because the DR1 peak in the UV−vis spectra was hidden by the stronger absorption of the polymer. Miktoarm polymers **13** and **14** showed the best loading capacities, while **15** and **16** with smaller PS and PCL chains exhibited the lowest levels of DR1 encapsulation. The encapsulation studies suggest that larger PS and PCL arm lengths contribute to a higher DR1 loading, and this is in agreement with the notion that the higher volume fractions of the hydrophobic polymers facilitate higher loading of the hydrophobic dye DR1 within the micelles. Another contributing factor to the encapsulation results comes from the micelle size of DR1-loaded μ-stars. Polymers **12** and **15** had the smallest micelle size (157 and 164 nm) compared to the rest of the miktoarm polymers and showed either undetectable or minimal DR1 loading. On the other hand, the rest of the polymers had sizes in excess of

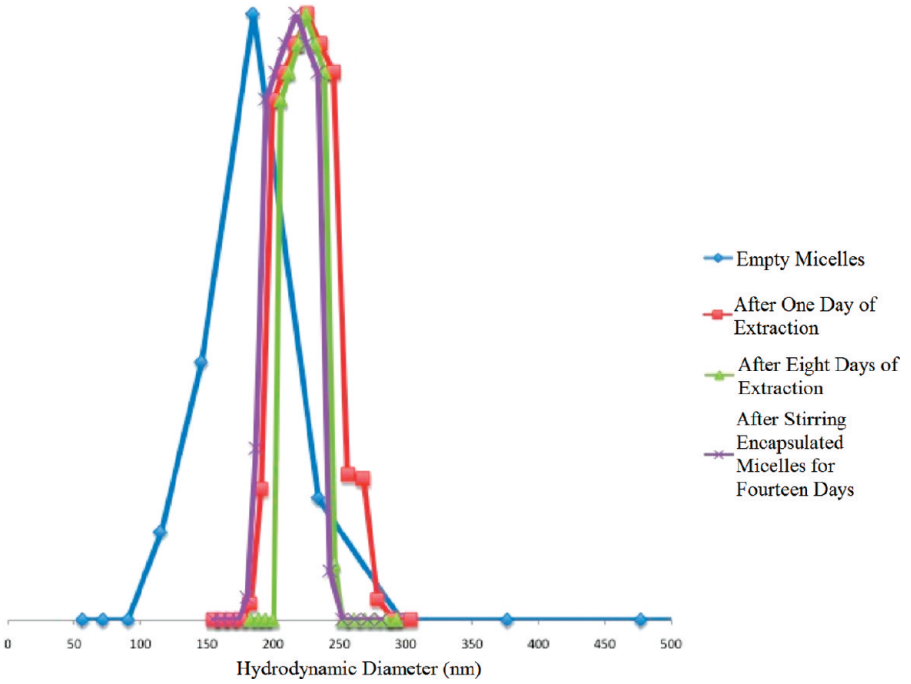

Figure 11. Evolution of size-distribution curve for DR1-loaded micelles of **11**, from initial DR1-loaded micelle preparation to prolonged exposure to the dye solution as well as vigorous stirring of the aqueous dye-loaded micelles for 2 weeks.

200 nm, corresponding to the systems that encapsulated more DR1. Finally, in predicting the loading capacity of a small molecule from the D_H in our systems, it is important to note that comparison of D_H of DR1-encapsulated polymers is more important than that of the blank aqueous micelles where the dye is absent. Even though our observations reveal that polymers above 200 nm typically show relatively high loading capacities, it is not easy to predict successful loading of small molecules based on the blank aqueous micelles due to changes that may take place in the micelle as it accommodates a small molecule within its hydrophobic interior.

Conclusions

We have demonstrated that well-defined ABC-type miktoarm star polymers can be synthesized using a highly versatile core with three orthogonal functionalities. Using this building block, we constructed a variety of μ-stars using a combination of highly efficient "click" chemistry reactions with ring-opening polymerization. The buildup of the ABC-type miktoarm polymers on the core molecule is easily monitored using simple techniques including ^{1}H, ^{13}C{^{1}H} NMR, and GPC. The star polymers containing PEG, PS, and PCL arms were found to assemble into spherical micelles in an aqueous solution in which the hydrophobic arms formed the core, while the hydrophilic PEG as corona interacted with the surrounding medium. Our results suggest that one could tailor the sizes of these aqueous micelles by varying the lengths of the appropriate polymeric arms. For instance, decreasing the size of the PEG arm led to an increase in both the core and the hydrodynamic diameter of the micelle. Also, increase in the hydrophobic PCL arm size led to increased micellar core sizes. Disperse Red 1 dye molecules were then encapsulated into the hydrophobic core of these micelles, and their loading capacity seemed to be dependent on the hydrodynamic diameter of the micelles as well as the length of the hydrophobic arms.

Experimental Section

Materials and Methods. ε-Caprolactone (Sigma-Aldrich, ≥99%) was dried over calcium hydride for 24 h and distilled under reduced pressure prior to use. Monohydroxy-terminated polystyrene was purchased from Scientific Polymer. Triisopropylsilylacetylene and trimethylsilylacetylene were purchased from Oakwood Chemicals, and 3-bromo-5-iodobenzoic acid was purchased from AK Scientific and used as received. Triethylamine and diethylamine were dried over potassium hydroxide and distilled prior to use. All reactions were performed under a nitrogen atmosphere using dried and distilled solvents. All other reagents were used as received. ^{1}H and ^{13}C{^{1}H} NMR spectra were recorded in $CDCl_3$ at ambient temperature using either a 400 or 500 MHz Varian instrument. Gel permeation chromatography (GPC) was performed in THF at 30 °C on a Viscotek TDA model 301 triple detector array equipped with a refractive index detector that was calibrated with polystyrene standards. The instrument was also equipped with two PolyAnalytik columns (PAS-103M-L and PAS-104M-M). The flow rate was 1 mL/min. Mass spectra were recorded on Thermo Scientific Orbitrap mass analyzer (ES) and Kratos MS25 (EI) mass spectrometers.

UV−vis spectra were obtained from a Cary 5000 spectrophotometer in 1 cm cuvettes. First, a calibration curve was constructed for DR1 dissolved in DCM by creating a series of solutions of DR1 with known concentrations (3 mL). After recording the absorbances of these solutions (in the range of 1−8 μg/mL), a line of best fit was constructed in order to model the relationship between the concentration of DR1 in DCM and its absorbance. The obtained calibration curve was deemed accurate as the correlation coefficient r^2 value was 0.996. The dye-encapsulated polymer solutions were then lyophilized to obtain a reddish powder. These solutions were then dissolved in 3 mL of DCM, and their UV−vis absorbances were recorded. Using the calibration curve, the loading level of the dye was calculated from the following formula: wt % = (mass of DR1)/(mass of polymer and DR1 in solution) × 100.

Dynamic light scattering (DLS) measurements were carried out on a Brookhaven photon correlation spectrometer equipped with a BI9000 AT digital correlator. Also on this instrument is a compass 315M-150 laser (Coherent Technologies). Measurements were taken at a wavelength of 532 nm. Measurements were made at ~25 °C at a 90° scattering angle. Mean hydrodynamic radius measurements were obtained from a Gaussian

fit of the CONTIN analysis mode from five averaged measurements of the dilute dispersion.

Transmission electron microscopy (TEM) was used to capture images of the aqueous micelles using a Phillips CM200 electron microscope equipped with an AMT 2k × 2k CCD camera at an acceleration voltage of 80 kV. TEM samples were prepared by adding 2−3 drops of the aqueous micelle solutions onto a Formvar-coated 400 mesh grid stabilized with evaporated carbon film. The samples were stained with OsO_4. The samples were allowed to dry overnight at room temperature.

3-Bromo-5-iodobenzyl alcohol (**3a**) was synthesized from its carboxylic acid by adopting a literature procedure.[14]

Synthesis of 3-Bromo-5-(triisopropylsilylethynyl)benzyl Alcohol (***3***). To a solution of 3-bromo-5-iodobenzyl alcohol (5 g, 16 mmol) in diethylamine (150 mL), catalytic amounts (ca. 5 mol %) of $[Pd_2Cl_2(PPh_3)_2]$ and CuI were added. The solution was then degassed by three evacuation/refill cycles and placed under nitrogen, and triisopropylsilylacetylene (3.80 g, 20.8 mmol) was added via syringe. The reaction mixture was stirred at room temperature for 48 h. The solvent was then removed *in vacuo*, and the residue was extracted with diethyl ether. The extract was dried over $MgSO_4$, and the solvent was then removed *in vacuo*. The product was purified by silica gel column chromatography using an ethyl acetate/hexanes (1:20) mixture. The solvent was removed *in vacuo* to yield a pale yellow oil (4.64 g, 79.1%). ^{1}H NMR (400 MHz, $CDCl_3$): δ (ppm) 1.12 (s, 21H, $-Si(C_3H_7)_3$), 4.63 (d, 2H, $-ArCH_2OH$), 7.38 (d, 1H, Ar*H*), 7.45 (s, 1H, Ar*H*), 7.52 (s, 1H, Ar*H*). $^{13}C\{^1H\}$ NMR (75 MHz, $CDCl_3$): δ (ppm) 11.5, 18.9, 64.3, 92.7, 105.4, 122.4, 125.7, 129.0, 130.0, 133.9, and 143.1. HRMS (EI): Theoretical M_w = 366.10 g/mol. Found M_w = 366.10 g/mol.

Synthesis of 3-(Triisopropylsilylethynyl)-5-(trimethylsilylethynyl)benzyl Alcohol (***4***). To a solution of 3-bromo-5-(triisopropylsilylethynyl)benzyl alcohol (4.46 g, 12.2 mmol) in benzene (70 mL) and triethylamine (130 mL), catalytic amounts (ca. 5 mol %) of $[PdCl_2(PPh_3)_2]$ and CuI were added, and the reaction mixture was stirred to dissolution. The reaction flask was degassed by three evacuation/refill cycles and placed under nitrogen, after which trimethylsilylacetylene (3.58 g, 36.5 mmol) was added via syringe. The reaction mixture was stirred under reflux overnight. The solvent was then evaporated, and the residue was extracted with diethyl ether. The extract was dried over $MgSO_4$, and the solvent was again removed *in vacuo*. The product was purified by silica gel column chromatography using an ethyl acetate/hexanes (1:20) mixture. The solvent was removed under vacuum to yield a pale yellow oil (4.23 g, 90.4%). ^{1}H NMR (300 MHz, $CDCl_3$): δ (ppm) 0.23 (s, 9H, $Si(CH_3)_3$), 1.12 (s, 21H, $-Si(C_3H_7)_3$), 4.63 (d, 2H, $-ArCH_2OH$), 7.41 (s, 2H, Ar*H*), 7.50 (s, 1H, Ar*H*). $^{13}C\{^1H\}$ NMR (100 MHz, $CDCl_3$): δ (ppm) 0.1, 11.2, 18.6, 64.4, 91.5, 95.0, 103.9, 105.8, 123.5, 123.9, 130.0, 130.2, 134.4, and 141.1. HRMS (ESI): Theoretical M_w^+ = 385.23 g/mol. Found M_w^+ = 385.32 g/mol.

Azide-terminated poly(ethylene glycol) monomethyl ethers, $M_n \approx 775$ (**5a**) and $M_n \approx 2000$ (**5b**), were synthesized from their commercially available monohydroxy forms by adopting a literature procedure.[15]

Synthesis of Azide-Terminated Polystyrene, $M_w \approx 4-5000$ (***6b***). To a solution of commercially available monohydroxy-terminated polystyrene (20 g, 4.65 mmol) in dichloromethane (DCM, 100 mL) cooled to 0 °C in an ice bath, methanesulfonyl chloride (1.07 g, 9.30 mmol) and triethylamine (0.94 g, 9.30 mmol) were added in a dropwise fashion. The ice bath was subsequently removed, and the reaction mixture was warmed to room temperature over a period of 24 h while being continuously stirred. The reaction mixture was then washed thoroughly with water and dried over $MgSO_4$. Upon removal of the solvent *in vacuo*, a clear oil was obtained (19 g, 95%). The mesylate-terminated polystyrene (19 g, 4.42 mmol) was dissolved in DMF (100 mL) and heated to 50 °C, and sodium azide (1.44 g, 22.1 mmol) was added. The reaction mixture was stirred for 24 h. After letting the reaction mixture cool to room temperature, the product was extracted with DCM and washed thoroughly with water. The extract was then dried over $MgSO_4$, and the solvent was removed *in vacuo*. The residue was dissolved in THF (25 mL) and precipitated in cold methanol (500 mL). After vacuum filtration, the precipitate was dried under vacuum to yield a white powder (18.05 g, 95%). ^{1}H NMR (500 MHz, $CDCl_3$): δ (ppm) 1.3−2.2 (br), 2.89 (br), 6.3−7.2 (br). $^{13}C\{^1H\}$ NMR (125 MHz, $CDCl_3$): δ (ppm) 31.2, 40.5 (br), 44.0 (br), 49.1, 125.0 (br), 128.2 (br). GPC: M_n = 4300 g/mol, M_w/M_n = 1.040.

Synthesis of 3-(Triisopropylsilyl)-5-ethynylbenzyl Alcohol (***7***). A solution of 3-(triisopropylsilylethynyl)-5-(trimethylsilylethynyl)benzyl alcohol (1.69 g, 4.4 mmol) in acetone (20 mL) was prepared and stirred for ∼15 min at room temperature. Subsequently, an aqueous solution of K_2CO_3 (10 mL; 1.4 g, 7.89 mmol) was added. The reaction mixture was left to stir overnight at room temperature. After acetone was removed *in vacuo*, the solution was extracted with DCM. The extract was dried over $MgSO_4$, and the solvent was removed under vacuum. The residue was then purified by silica gel column chromatography using an ethyl acetate/hexanes (1:4) mixture, and the solvent was again evaporated to yield a yellowish oil (1.12 g, 81%). ^{1}H NMR (400 MHz, $CDCl_3$): δ (ppm) 1.12 (s, 21H, $-Si(C_3H_7)_3$), 1.78 (s, 1H, $-CH_2OH$), 3.08 (s, 1H, $-ArCCH$), 4.66 (d, 2H, CH_2OH), 7.30 (s, 1H, Ar*H*), 7.45 (s, 1H, Ar*H*), 7.53 (s, 1H, Ar*H*). $^{13}C\{^1H\}$ NMR (75 MHz, $CDCl_3$): δ (ppm) 11.5, 18.8, 64.5, 78.1, 82.8, 91.9, 105.9, 122.7, 124.3, 130.3, 130.8, 134.9, and 141.4.

Typical "Click" Reaction of PEG-N_3 to the Deprotected Alkyne, $M_n \approx 2000$ (***8***). CuBr (0.116 g, 0.807 mmol) was added to a solution of PEG-N_3 (1.366 g, 0.632 mmol) in *N,N*-dimethylformamide (DMF) (10 mL) in a Schlenk flask. The solution was degassed by three evacuation/refill cycles and placed under nitrogen, after which a second solution of 3-(triisopropylsilylethynyl)-5-ethynylbenzyl alcohol (0.202 g, 0.645 mmol) in DMF (5 mL) was added. Upon complete dissolution of the reactants, the flask was further degassed by three additional evacuation/refill cycles. Nitrogen-purged *N,N,N′,N″,N″*-pentamethyldiethylenetriamine (PMDETA) (0.140 g, 0.807 mmol) was then added, whereupon the reaction mixture developed a dark green color. The solution was stirred at room temperature for 24 h. Aliquots were periodically removed for analysis by GPC. After the reaction, the solution was exposed to air and DMF was removed under vacuum. Upon dilution with DCM, the solution was passed through a silica gel column to remove the copper catalyst and the unreacted starting materials using a methanol/DCM (1:20) mixture as eluent. Then, the solvent was removed, and the solution was dried under vacuum to yield a light-brown gel (1.437 g, 92%). ^{1}H NMR (400 MHz, $CDCl_3$): δ (ppm) 1.13 (s, 23H, $-Si(C_3H_7)_3$), 2.63 (t, 1H, $-CH_2OH$), 3.37 (s, 3H, $-PEG-OCH_3$), 3.49−3.65 (br, PEG), 3.91 (t, 2H, $-PEG-CH_2-CH_2-TriAz-$), 4.60 (t, 2H, $-PEG-CH_2-CH_2-TriAz-$), 4.71 (d, 2H, $-ArCH_2OH$), 7.43 (s, 1H, Ar*H*), 7.80 (s, 1H, Ar*H*), 7.93 (s, 1H, Ar*H*), 8.12 (s, 1H, TriAz−*H*). $^{13}C\{^1H\}$ NMR (125 MHz, $CDCl_3$): δ (ppm) 11.3, 18.7, 30.3, 50.4, 59.0, 64.4, 69.4, 70.5, 71.9, 90.8, 106.6, 121.6, 124.0, 124.2, 128.0, 129.8, 131.1, 142.0, and 146.8. GPC: M_n = 3485 g/mol. M_w/M_n = 1.031.

A similar procedure was followed for the "click" reaction using azide-terminated poly(ethylene glycol) monomethyl ether with $M_n \approx 775$.

Removal of Triisopropylsilyl (TIPS) Protecting Group (***9***). A flask containing a solution of **8** (1.35 g, 0.546 mmol) in THF (25 mL) was placed in a dry ice/acetone bath. After waiting 15 min for the solution to cool to approximately −78 °C, a solution of Bu_4NF (1.0 M solution in THF, 1.162 mL, 1.162 mmol) was added in a dropwise fashion. The bath was then removed, and the reaction mixture was allowed to warm to room temperature while stirring overnight. After removing the solvent under vacuum, the solution was extracted into DCM. After drying the extract over $MgSO_4$ and removing the solvent *in vacuo*, the residue was thoroughly washed with hexanes (300 mL) to yield a brown gel (1.012 g, 80%). ^{1}H NMR

(400 MHz, $CDCl_3$): δ (ppm) 3.12 (s, 1H, −ArCC*H*), 3.37 (s, 3H, −PEG−OCHH_3), 3.54−3.65 (br, PEG), 3.90 (t, 1H, −PEG−CH_2−CH_2−TriAz−), 4.60 (t, 2H, −PEG−CH_2−CH_2−TriAz−), 4.71 (s, 2H, −ArCH_2OH), 7.44 (s, 1H, Ar*H*), 7.88 (s, 1H, Ar*H*), 7.92 (s, 1H, Ar*H*), 8.13 (s, 1H, TriAz−*H*). $^{13}C\{^1H\}$ NMR (125 MHz, $CDCl_3$): δ (ppm) 30.9, 50.4, 59.0, 64.4, 69.4, 70.5, 71.9, 77.5, 83.3, 121.5, 122.8, 124.4, 128.2, 129.7, 131.3, 142.3, and 146.7. GPC: M_n = 3151 g/mol. M_w/M_n = 1.041.

Typical Procedure for "Click" Reaction of PS-N_3 with the Deprotected Alkyne for Addition of the Second Arm (***10***). CuBr (0.068 g, 0.475 mmol) was added to a DMF solution (10 mL) of **2** (0.880 g, 0.380 mmol) in a Schlenk flask. After subsequent addition of the azide-terminated polystyrene (1.634 g, 0.380 mmol, $M_n \approx 4300$), the solution was degassed by three evacuation/refill cycles and stirred to complete dissolution under nitrogen. Then, nitrogen-purged PMDETA (0.082 g, 0.475 mmol) was added whereupon the reaction mixture developed a dark green color. The solution was stirred at room temperature for 24 h while aliquots were periodically removed for analysis by GPC. The solution was then exposed to air and DMF was removed *in vacuo*. Upon dilution with DCM, the solution was passed through a silica gel column to remove both the copper catalyst and the unreacted starting materials using a methanol/DCM (1:20) mixture as eluent. The solvent was then removed, and the solution was dried under vacuum to yield a brown oil (1.91 g, 83%). ^1H NMR (500 MHz, $CDCl_3$): δ (ppm) 1.4−2.1 (br, PS), 3.38 (s, 3H, −PEG−OCHH_3), 3.54−3.64 (br, PEG), 3.90 (t, 2H, −PEG−CH_2−CH_2−TriAz−), 4.60 (t, 2H, −PEG−CH_2−CH_2−TriAz−), 4.8 (s, 1H, −ArCH_2OH), 6.3−7.2 (br, PS). $^{13}C\{^1H\}$ NMR (125 MHz, $CDCl_3$): δ (ppm) 13.7, 14.1, 19.8, 21.2, 22.6, 24.1, 29.4, 30.3, 31.6, 34.2, 40.3, 42−46, 50.4, 59.0, 69.4, 70.6, 71.9, 105.0, 123.5, 125−126, 126−128, 135.7, 145.3, and 151.5. GPC: M_n = 7261 g/mol. M_w/M_n = 1.055.

The same procedure was used for a "click" reaction with azide-terminated polystyrene with $M_n \approx 2700$.

Typical Procedure for the Ring-Opening Polymerization (ROP) of ε-Caprolactone To Form the Miktoarm Star (***11***). A solution of **3** (0.23 g, 0.036 mmol) in distilled toluene (10 mL) was added to a warm three-neck flask equipped with a condenser. After the solution was degassed by three evacuation/refill cycles, distilled ε-caprolactone (0.166 g, 1.456 mmol, $[CL]_0/[I]_0$ = 40) was added via syringe through a rubber septa, and the solution was warmed to 100 °C. A nitrogen-purged solution of Sn(II) 2-ethylhexanoate (3 mg, 7.28 μmol) in toluene (1 mL) was then added via syringe through a rubber septa, and the reaction mixture was warmed to 130 °C, stirring for ∼20 h. Aliquots were periodically removed for analysis by GPC. The reaction mixture was then cooled to room temperature, dissolved in DCM, and precipitated in cold methanol under vigorous stirring. After vacuum filtration, the precipitate was dried under vacuum to constant weight to yield an off-white powder (0.350 g, 70%). ^1H NMR (400 MHz, $CDCl_3$): δ (ppm) 1.38 (m, PCL), 1.63 (m, PCL), 1.3−2 (br, PS), 2.304 (t, PCL), 3.38 (s, 3H, −PEG−OCHH_3), 3.54−3.64 (br, PEG), 4.05 (t, PCL), 6.3−7.2 (br, PS). $^{13}C\{^1H\}$ NMR (75 MHz, $CDCl_3$): δ (ppm) 24.8, 25.7, 28.6, 34.3, 40.6, 64.4, 70.7, 125.9, 127 (br), and 173.8. GPC: M_n = 11 500 g/mol. M_w/M_n = 1.26.

Miktoarm Star (***12***). ^1H NMR (400 MHz, $CDCl_3$): δ (ppm) 1.40 (m, PCL), 1.63 (m, PCL), 1.3−2 (br, PS), 2.317 (t, PCL), 3.38 (s, 3H, −PEG−OCHH_3), 3.61−3.65 (br, PEG), 4.06 (t, PCL), 6.3−7.2 (br, PS). $^{13}C\{^1H\}$ NMR (75 MHz, $CDCl_3$): δ (ppm) 24.5, 25.3, 28.5, 34.3, 40.6, 64.0, 70.3, 126.1, 127 (br), and 173.8. GPC: M_n = 15 200 g/mol. M_w/M_n = 1.43.

Miktoarm Star (***13***). ^1H NMR (400 MHz, $CDCl_3$): δ (ppm) 1.38 (m, PCL), 1.63 (m, PCL), 1.3−2 (br, PS), 2.305 (t, PCL), 3.376 (s, 3H, −PEG−OCHH_3), 3.60−3.65 (br, PEG), 4.057 (t, PCL), 6.3−7.2 (br, PS). $^{13}C\{^1H\}$ NMR (75 MHz, $CDCl_3$): δ (ppm) 24.6, 25.5, 28.3, 34.1, 40.3, 64.1, 70.5, 125.6, 127 (br), and 173.5. GPC: M_n = 10 000 g/mol. M_w/M_n = 1.43.

Miktoarm Star (***14***). ^1H NMR (400 MHz, $CDCl_3$): δ (ppm) 1.38 (m, PCL), 1.64 (m, PCL), 1.3−2 (br, PS), 2.303 (t, PCL), 3.373 (s, 3H, −PEG−OCHH_3), 3.54−3.64 (br, PEG), 4.057 (t, PCL), 6.3−7.2 (br, PS). $^{13}C\{^1H\}$ NMR (75 MHz, $CDCl_3$): δ (ppm) 24.7, 25.8, 28.7, 34.3, 40.3, 64.4, 70.7, 125.9, 127 (br), and 174.0. GPC: M_n = 15 000 g/mol. M_w/M_n = 1.59.

Miktoarm Star (***15***). ^1H NMR (400 MHz, $CDCl_3$): δ (ppm) 1.43 (m, PCL), 1.67 (m, PCL), 1.3−2 (br, PS), 2.309 (t, PCL), 3.377 (s, 3H, −PEG−OCHH_3), 3.54−3.64 (br, PEG), 4.06 (t, PCL), 6.3−7.2 (br, PS). $^{13}C\{^1H\}$ NMR (75 MHz, $CDCl_3$): δ (ppm) 24.5, 25.4, 29.0, 34.2, 40.6, 64.4, 70.6, 125.8, 127 (br), and 174.2. GPC: M_n = 6500 g/mol. M_w/M_n = 1.28.

Miktoarm Star (***16***). ^1H NMR (400 MHz, $CDCl_3$): δ (ppm) 1.38 (m, PCL), 1.63 (m, PCL), 1.3−2 (br, PS), 2.304 (t, PCL), 3.38 (s, 3H, −PEG−OCHH_3), 3.54−3.64 (br, PEG), 4.05 (t, PCL), 6.3−7.2 (br, PS). $^{13}C\{^1H\}$ NMR (75 MHz, $CDCl_3$): δ (ppm) 24.8, 25.7, 28.6, 34.3, 40.6, 64.4, 70.7, 125.9, 127 (br), and 173.8. GPC: M_n = 10 900 g/mol. M_w/M_n = 1.55.

Preparation of Aqueous Micelles. Micelles of miktoarm polymers were prepared by a dialysis method using a known literature procedure.[21] In a typical procedure, 10 mg of the miktoarm polymer was dissolved in 1 mL of DMF and stirred for ∼30 min. Using a syringe pump, 10 mL of Milli-Q water was added dropwise to the DMF solution under vigorous stirring at the rate of one drop every 12 s. Afterward, the DMF was removed by dialysis against 2 L of Milli-Q water over a period of 24−48 h. The water was periodically replaced at least five times throughout the dialysis in order to ensure removal of DMF from solution.

Preparation of Dye-Encapsulated Aqueous Micelle Solutions. Two different methods were followed for the preparation of dye-encapsulated aqueous micelles of miktoarm polymers.

Extraction. The aqueous micelles already prepared from dialysis were used for the encapsulation of Disperse Red 1. To the solution, as described above, ca. 4 mL of a concentrated solution of DR1 in *tert*-butyl methyl ether (1 mg/mL) was added and stirred vigorously overnight. This concentration was chosen to ensure an abundance of DR1 throughout the extraction. Afterward, the solution was allowed to fully separate into two phases, and the aqueous layer was withdrawn from the solution.

Dialysis. In this method, the preparation of micelles encapsulated with Disperse Red 1 was similar to that described for the preparation of aqueous micelles. The only difference was that ca. 5 mg of DR1 was added in addition to the polymer, prior to dissolution in DMF. This amount was chosen to ensure an abundance of DR1 so that the self-assembled polymers can encapsulate as much DR1 as possible.

Acknowledgment. We thank NSERC of Canada and Center for Self-Assembled Chemical Structures (FQRNT, Quebec Canada) for financial assistance.

Supporting Information Available: GPC data profiles for the miktoarm polymers. This material is available free of charge via the Internet at http://pubs.acs.org.

References and Notes

(1) (a) Hadjichristidis, N. *J. Polym. Sci., Part A: Polym. Chem.* **1999**, *37*, 857–871. (b) Khanna, K.; Varshney, S.; Kakkar, A. *Polym. Chem.* **2010**, DOI: 10.1039/c0py00082e.
(2) Hadjichristidis, N.; Pitsikalis, M.; Pispas, S.; Iatrou, H. *Chem. Rev.* **2001**, *101*, 3747–3792.
(3) Glauser, T.; Stancik, C. M.; Moller, M.; Voytek, S.; Gast, A. P.; Hedrick, J. L. *Macromolecules* **2002**, *35*, 5774–81.
(4) (a) Bernaerts, K. V.; Du Prez, F. E. *Prog. Polym. Sci.* **2006**, *31*, 671–722. (b) Fragouli, P.; Iatrou, H.; Hadjichristidis, N.; Sakurai, T.; Matsunaga, Y.; Hirao, A. *J. Polym. Sci., Part A: Polym. Chem.* **2006**, *44*, 6587–99.
(5) (a) Yamazaki, Y.; Ajioka, N.; Yokoyama, A.; Yokozawa, T. *Macromolecules* **2009**, *42*, 606–611. (b) Wang, G.; Huang, J. *J. Polym. Sci., Part A: Polym. Chem.* **2008**, *46*, 1136–1150. (c) Wiltshire, J. T.;

Qiao, G. G. *Macromolecules* **2006**, *39*, 9018–27. (d) Hadjichristidis, N.; Iatrou, H.; Pitsikalis, M.; Pispas, S.; Avgeropoulos, A. *Prog. Polym. Sci.* **2005**, *30*, 725–782. (e) He, T.; Li, D. J.; Sheng, X.; Zhao, B. *Macromolecules* **2004**, *37*, 3128–3135. (f) Nasser-Eddine, M.; Reutenauer, S.; Delaite, C.; Hurtrez, G.; Dumas, P. J. *J. Polym. Sci., Part A: Polym. Chem.* **2004**, *42*, 1745–1751. (g) Li, Z. B.; Hillmyer, M. A.; Lodge, T. P. *Macromolecules* **2004**, *37*, 8933–8940. (h) Feng, X. S.; Pan, C. Y. *Macromolecules* **2002**, *35*, 4888–93. (i) Heise, A.; Trollsas, M.; Magbitang, T.; Hedrick, J. L.; Frank, C. W.; Miller, R. D. *Macromolecules* **2001**, *34*, 2798–804. (j) Bellas, V.; Iatrou, H.; Hadjichristidis, N. *Macromolecules* **2000**, *33*, 6993–6997. (k) Gao, H.; Matyjaszewski, K. *J. Am. Chem. Soc.* **2007**, *129*, 11828–11834. (l) Heise, A.; Trollsas, M.; Magbitang, T.; Hedrick, J. L.; Frank, C. W.; Miller, R. D. *Macromolecules* **2001**, *34*, 2798–2804. (m) Gao, H.; Tsarevsky, N. V.; Matyjaszewski, K. *Macromolecules* **2005**, *38*, 5995–6004. (n) Altintas, O.; Hizal, G.; Tunca, U. *J. Polym. Sci., Part A: Polym. Chem.* **2006**, *44*, 5699–5707.

(6) (a) Kolb, H. C.; Finn, M. G.; Sharpless, K. B. *Angew. Chem., Int. Ed.* **2001**, *40*, 2004–21. (b) Franc, G.; Kakkar, A. *Chem. Commun.* **2008**, 5267–5276. (c) Franc, G.; Kakkar, A. K. *Chem.—Eur. J.* **2009**, *15*, 5630–5639. (d) Franc, G.; Kakkar, A. K. *Chem. Soc. Rev.* **2010**, *39*, 1536–1544.

(7) (a) Vora, A.; Singh, K.; Webster, D. C. *Polymer* **2009**, *50*, 2768–2774. (b) Whittaker, M. R.; Urbani, C. N.; Monterio, M. J. *J. Am. Chem. Soc.* **2006**, *128*, 12360.

(8) (a) Zhang, S.; Du, J.; Sun, R.; Li, X.; Yang, D.; Zhang, S. *React. Funct. Polym.* **2003**, *56*, 17–25. (b) Chen, S.; Pieper, R.; Webster, D. C.; Singh, J. *Int. J. Pharm.* **2005**, *288*, 207–18.

(9) (a) Mavroudis, A.; Avgeropoulos, A.; Hadjichristidis, N.; Thomas, E. L.; Lohes, D. J. *Chem. Mater.* **2003**, *15*, 1976. (b) Teslikas, Y.; Iatrou, H.; Hadjichristidis, N.; Liang, K. S.; Mohanty, K.; Lohse, D. J. *J. Chem. Phys.* **1996**, *105*, 2456.

(10) (a) Babin, J.; Taton, D.; Brinkmann, M.; Lecommandoux, S. *Macromolecules* **2008**, *41*, 1384. (b) Babin, J.; Leroy, C.; Lecommandoux, S.; Borsali, R.; Gnanou, Y.; Taton, D. *Chem. Commun.* **2005**, 1993.

(11) (a) Li, Z. B.; Hillmyer, M. A.; Lodge, T. P. *Langmuir* **2006**, *22*, 9409–9417. (b) Li, Z. B.; Hillmyer, M. A.; Lodge, T. P. *Nano Lett.* **2006**, *6*, 1245–1249. (c) Li, Z. B.; Hillmyer, M. A.; Lodge, T. P. *Macromolecules* **2006**, *39*, 765–771. (d) Li, Z. B.; Kesselman, E.; Talmon, Y.; Hillmyer, M. A.; Lodge, T. P. *Science* **2004**, *306*, 98–101.

(12) Saito, N.; Liu, C.; Lodge, T. P.; Hillmyer, M. A. *Macromolecules* **2008**, *41*, 8815–8822.

(13) Valverde, I. E.; Delmas, A. F.; Aucagne, V. *Tetrahedron* **2009**, *65*, 7597–7602.

(14) Lehmann, U.; Schlüter, A. D. *Eur. J. Org. Chem.* **2000**, 3483–3489.

(15) Gao, H.; Matyjaszewski, K. *J. Am. Chem. Soc.* **2007**, *129*, 6633–6639.

(16) van Dijk, M.; Nollet, M. L.; Weijers, P.; Dechesne, A. C.; van Nostrum, C. F.; Hennink, W. E.; Dirk, T. S.; Rijkers, D. T. S.; Liskamp, R. M. J. *Biomacromolecules* **2008**, *9*, 2834–2843.

(17) Rieger, J.; Coulembier, O.; Dubois, P.; Bernaerts, K. V.; Du Prez, F. E.; Jérôme, R.; Jérôme, C. *Macromolecules* **2005**, *38*, 10650–10657.

(18) Liu, H.; Li, C.; Liu, H.; Liu, S. *Langmuir* **2009**, *25*, 4724–4734.

(19) Liu, H.; Li, C.; Liu, H.; Liu, S. *Langmuir* **2009**, *25*, 4724–4734.

(20) Fox, M. E.; Szoka, F. C.; Fréchet, J. M. J. *Acc. Chem. Res.* **2009**, *42*, 1141–1151.

(21) Zhang, L.; Eisenberg, A. *J. Am. Chem. Soc.* **1996**, 3168–3181.